

CASE FILE
COPY

NACA TN 4077

NATIONAL ADVISORY COMMITTEE
FOR AERONAUTICS

TECHNICAL NOTE 4077

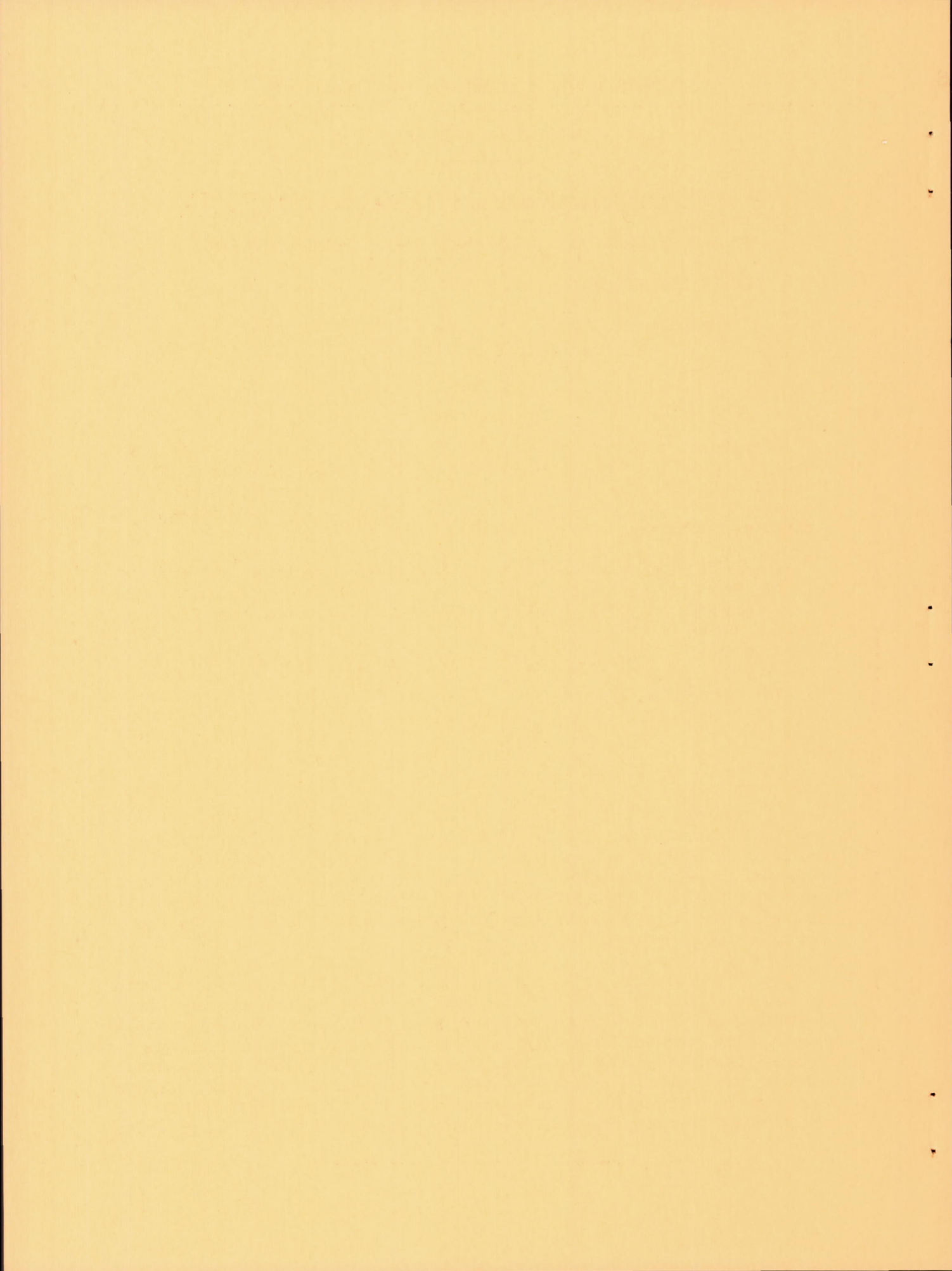
STATIC LONGITUDINAL AND LATERAL STABILITY
CHARACTERISTICS AT LOW SPEED OF 45° SWEPTBACK-MIDWING
MODELS HAVING WINGS WITH AN ASPECT RATIO OF 2, 4, OR 6

By David F. Thomas, Jr., and Walter D. Wolhart

Langley Aeronautical Laboratory
Langley Field, Va.



Washington
September 1957



S

NATIONAL ADVISORY COMMITTEE FOR AERONAUTICS

TECHNICAL NOTE 4077

STATIC LONGITUDINAL AND LATERAL STABILITY

CHARACTERISTICS AT LOW SPEED OF 45° SWEPTBACK-MIDWING

MODELS HAVING WINGS WITH AN ASPECT RATIO OF 2, 4, OR 6

By David F. Thomas, Jr., and Walter D. Wolhart

SUMMARY

A systematic investigation was conducted in the Langley stability tunnel to determine the effects of the various components and combinations of components on the static longitudinal and lateral stability characteristics at low speed of a series of 45° sweptback-midwing-airplane configurations having wings with an aspect ratio of 2, 4, or 6.

The results of this investigation have indicated that the wing-on tail effectiveness in producing negative pitching moment increased with aspect ratio and angle of attack and became approximately equal to the wing-off value at very high angles of attack. Also, all complete models tested became directionally unstable in the high angle-of-attack range primarily as a result of increased losses in the stable contribution of the tail both with angle of attack and increasing wing aspect ratio.

INTRODUCTION

In general, at low angles of attack satisfactory estimates of the stability characteristics of midwing or near-midwing airplanes having bodies of revolution may be made by use of procedures such as those presented in reference 1. At moderate to high angles of attack, however, reliable estimates are difficult, if not impossible, to make because of the unpredictable interference effects between the various components of the airplane.

Experimental data are available from a number of sources concerning the static stability characteristics of the unswept-wing case and the swept-wing case (for example, refs. 2 to 8). These data show the influence of such geometric variables as tail area, tail length, fuselage cross section, wing location, and others. The effects of wing aspect ratio on the stability characteristics for wing-alone and wing-fuselage configurations are given in references 9 to 13. Little systematic information, however, is available concerning the effect of wing aspect

ratio on the contributions of wings, fuselages, and tails to the stability characteristics of complete models. In order to provide this information an investigation (ref. 2) was conducted in the Langley stability tunnel on a series of unswept-midwing models having interchangeable wings of aspect ratio 2, 4, or 6.

The purpose of the present paper is to extend the results of the unswept-wing investigation of reference 2 to include the static longitudinal and lateral stability characteristics for a series of 45° sweptback-midwing configurations with wings of aspect ratio 2, 4, or 6. Data are presented for an angle-of-attack range from -4° to 32° . The effects of wing aspect ratio on the contributions of the various components to the static longitudinal and lateral stability characteristics are presented with particular emphasis on the influence of the components, singly and in combination, on the tail contributions.

SYMBOLS

All data are referred to the stability system of axes with the origin at the projection on the plane of symmetry of the quarter-chord point of the wing mean aerodynamic chord. Positive directions of forces, moments, and angular displacements are shown in figure 1. The coefficients and symbols are defined as follows:

A aspect ratio, $\frac{b^2}{S}$

b span, ft

c local chord, ft

\bar{c} mean aerodynamic chord, $\frac{2}{S} \int_0^{b/2} c^2 dy$, ft

l tail length, distance measured parallel to fuselage reference line from mounting point to $\bar{c}/4$ of the tail (same for vertical and horizontal tail), ft

S surface area, sq ft

x location of quarter-chord point of local chord, measured from leading edge of root chord parallel to chord of symmetry, ft

\bar{x} location of quarter-chord point of mean aerodynamic chord, measured from leading edge of root chord parallel to chord

of symmetry, $\frac{2}{S} \int_0^{b/2} cx dy$, ft

y	spanwise distance measured from and perpendicular to plane of symmetry, ft
\bar{y}	spanwise distance to mean aerodynamic chord, measured from and perpendicular to plane of symmetry, $\frac{2}{S} \int_0^{b/2} c_y dy$, ft
z	spanwise distance along vertical tail measured from and perpendicular to fuselage reference line, ft
\bar{z}	spanwise distance along vertical tail to mean aerodynamic chord of vertical tail, measured from and perpendicular to fuselage reference line, $\frac{1}{S_v} \int_0^{b_v} c_z dz$, ft
q	free-stream dynamic pressure, $\frac{1}{2} \rho V^2$, lb/sq ft
V	free-stream velocity, ft/sec
v	spanwise component of free-stream velocity, ft/sec
ρ	density, slugs/cu ft
α	angle of attack, deg
β	angle of sideslip, defined as $\sin^{-1} \frac{v}{V}$, deg
C_D'	approximate drag coefficient, $\frac{\text{Drag}}{q S_w}$
C_L	lift coefficient, $\frac{\text{Lift}}{q S_w}$
C_Y	side-force coefficient, $\frac{\text{Side force}}{q S_w}$
C_m	pitching-moment coefficient, $\frac{\text{Pitching moment}}{q S_w \bar{c}_w}$
C_n	yawing-moment coefficient, $\frac{\text{Yawing moment}}{q S_w b_w}$
C_r	rolling-moment coefficient, $\frac{\text{Rolling moment}}{q S_w b_w}$

$$C_{Y\beta} = \frac{\partial C_Y}{\partial \beta} \text{ per degree}$$

$$C_{n\beta} = \frac{\partial C_n}{\partial \beta} \text{ per degree}$$

$$C_{l\beta} = \frac{\partial C_l}{\partial \beta} \text{ per degree}$$

Subscripts:

h horizontal tail

r root

t tip

v vertical tail

VH contribution of the combination of vertical and horizontal tails to various force and moment coefficients

w wing

Model component designations:

W wing alone

F fuselage alone

VH combination of vertical and horizontal tails, always tested as a unit (tail alone)

WF wing-fuselage combination

WVH wing-tail combination

FVH fuselage-tail combination

WFVH wing-fuselage-tail combination (complete model)

Nomenclature used to denote configurations involved in the method of subtracting the data of various configurations to obtain the contribution of the vertical-tail—horizontal-tail assembly to the various force and moment coefficients is as follows:

FVH-F	fuselage-tail combination minus fuselage alone
WVH-W	wing-tail combination minus wing alone
WFVH-WF	complete model minus wing-fuselage combination

APPARATUS AND MODELS

This investigation was made in the 6-foot-diameter test section of the Langley stability tunnel. The models were mounted on a single support strut which was in turn fastened to a six-component electromechanical balance system.

The models were constructed primarily of laminated mahogany with Inconel and aluminum-alloy stiffeners in the wing and tail surfaces. Geometric characteristics of the models are presented in table I; the principle dimensions of the complete models are shown in figure 2. Sketches of the plan forms of the three 45° sweptback wings of aspect ratios 2, 4, and 6 used in this investigation are shown in figure 3. Ordinates of the fuselage and the NACA 65A008 airfoil section used for the wings and tail surfaces are presented in table II. The fuselage was circular in cross section in planes perpendicular to the fuselage reference line.

In this investigation the horizontal and vertical tails were tested as a unit at all times. In the absence of the fuselage, the tail group was mounted on a boom in the same position relative to the mounting point ($c/4$ of the wing) that the tail occupied in the presence of the fuselage. A complete-model configuration and a wing-tail configuration mounted on a single-strut support are shown in figure 4.

TESTS AND CORRECTIONS

Tests for this investigation were made at a dynamic pressure of 24.9 pounds per square foot which corresponds to a Mach number of 0.13. The Reynolds numbers based on the wing mean aerodynamic chord were 1.00×10^6 for the aspect-ratio-2 wing, 0.71×10^6 for the aspect-ratio-4 wing, and 0.58×10^6 for the aspect-ratio-6 wing.

The longitudinal characteristics C_m , C_L , and C_D' were determined for an angle-of-attack range of -4° to 32° . The sideslip derivatives $C_{Y\beta}$, $C_{n\beta}$, and $C_{l\beta}$ were determined for this range of angle of attack by using values for angle of sideslip of 5° and -5° .

The angle of attack, the drag coefficient, and the pitching-moment coefficient have been corrected for jet-boundary effects by using approximate corrections based on unswept-wing theory and in the manner suggested in references 14 and 15. Tare corrections have been applied only to the wing-on basic longitudinal data C_m , C_L , and C_D' . The data have not been corrected for blockage.

PRESENTATION OF RESULTS

The results of this investigation are presented as coefficients of forces, moments, and derivatives plotted against angle of attack for the various model configurations. A summary of the configurations investigated and of the figures that present the data for these configurations, together with the purpose of these figures, is given in the following table:

Data (plotted against α)	Configuration	Figure	Purpose of figure to show -
C_m , C_L , C_D'	W, WF, WVH, WFVH	5	Effect of the various model components singly and in combination on the basic longitudinal data.
	F, VH, FVH	6	
$(C_L)_{VH}$	VH, FVH-F, WVH-W, WFVH-WF	7	Effect of the various model components on the tail contribution to longitudinal stability.
		8	
$(C_m)_{VH} \frac{c_w}{l}$	VH, FVH-F, WVH-W, WFVH-WF	9	Effect of wing aspect ratio on the tail contribution to longitudinal stability with and without the fuselage.
$C_{Y\beta}$, $C_{n\beta}$, $C_{l\beta}$	W, WF, WVH, WFVH	10	Effect of the various model components singly and in combination on the static lateral derivatives.
	F, VH, FVH	11	
$(C_{Y\beta})_{VH}$	VH, FVH-F, WVH-W, WFVH-WF	12	Effect of the various model components on the tail contribution to the static lateral derivatives.
$(C_{n\beta})_{VH}$		13	
$(C_{l\beta})_{VH}$		14	
$(C_{n\beta})_{VH} \frac{b_w}{l}$		15	Effect of wing aspect ratio on the tail contribution to directional stability with and without the fuselage.

DISCUSSION

Preliminary Remarks

Interpretation of the results of this investigation may be misleading in that the characteristic lengths \bar{c}_w and b_w change with wing aspect ratio (the wing area remains constant) and, of course, this change results in a given moment being transformed into a different coefficient for each aspect ratio. Examples of the possible misinterpretation of data may be noted in figure 6 or figure 11, wherein data are presented for the wing-off configurations for the three different aspect ratios. These data are actually the same but, when they are reduced to coefficient form by use of the appropriate values of \bar{c}_w and b_w , the moment data form three different curves for each original curve. In order to eliminate this apparent effect of wing aspect ratio on the tail contributions to pitching moment $(C_m)_{VH}$ and directional stability $(C_{n\beta})_{VH}$, plots are provided in which the tail length l is used in place of \bar{c}_w and b_w as the characteristic dimension. (See figs. 9 and 15.) This problem is not present in the force data due to the fact that the area used to reduce these data was the same for all wing aspect ratios.

Static Longitudinal Stability Characteristics

Basic static longitudinal stability characteristics.—The expected trends for swept wings alone (ref. 10), i.e., increasing lift-curve slope at 0° angle of attack with increasing aspect ratio and increasing lift-curve slope with angle of attack, up to approximately an angle of attack of 12° , for the wings of aspect ratios 2 and 4, are present in the results for the models tested in this investigation (fig. 5). Likewise, the presence of pitch-up due to tip stall and its increased severity with increasing aspect ratio (see curves in fig. 5 for wing aspect ratios of 4 and 6) would be expected on the basis of the results of reference 10. The effect of increasing aspect ratio in reducing the angle of attack at which pitch-up occurs, indicated by the results for wings of aspect ratios 4 and 6, was similar to that shown in reference 11.

The complete models follow the trends in pitching moment established by their respective wings. The positive pitching-moment contribution of the fuselage alone is apparently cancelled to a large extent by the mutual interference of the wing and fuselage when the fuselage is tested in combination with wings of aspect ratios 4 and 6 (tail on or off). (See fig. 5.) This cancellation of the fuselage contribution is present for the models of aspect ratios 4 and 6 except at very high angles of attack.

The aspect-ratio-2 models, however, appear to retain to some degree the positive pitching-moment contribution of the fuselage throughout the angle-of-attack range investigated.

Tail contribution to pitching-moment coefficient. - Examination of figure 9 discloses a loss in the contribution of the tail to negative pitching moment when the tail was tested in the presence of the wings.

This loss in tail contribution $(C_m)_{VH} \frac{\bar{c}_w}{l}$ is a function of both angle of attack and wing aspect ratio and results from the variation in location of the wing wake with respect to the tail and to the local strength of the wing wake. The angle-of-attack variation in $(C_m)_{VH} \frac{\bar{c}_w}{l}$ obviously is due to the movement of the horizontal tail down and out of the wing wake. At a sufficiently high angle of attack the tail is out of the wake and, as seen in figure 9, the tail contribution is approximately equal to that of the wing-off configurations. The aspect-ratio variation may be assumed to arise because of three factors, all of which tend to produce the same results - i.e., increased downwash at the tail with decreasing aspect ratio which reduces the tail contribution to negative pitching moment. These factors are: the local downwash at the tail being increased by the wing effectively moving closer to the tail with decreasing wing aspect ratio, a greater proportion of the load being carried by the center section of the wings with decreasing aspect ratio (the local downwash behind the wing varies with the local wing load, increasing with increasing load), reference 10, and the decreased span of the wings with decreasing aspect ratio placing the trailing vortices closer inboard with respect to the tail.

The results of this investigation showed more definition in the effects of wing aspect ratio on the tail contribution to pitching moment than those for the unswept wings of reference 2, probably as a result of the leading-edge vortices of the swept wings being inboard of the tip. The effects of the fuselage on the tail contribution to pitching moment are negligible for these tests, and little of the effect of mutual interference of the wing and fuselage of the complete model on the tail contribution noted in reference 2 for the straight wings was found for these 45° swept wings.

Static Lateral Stability Characteristics

Basic static lateral stability characteristics. - Each of the three complete models (fig. 10) became directionally unstable in the high angle-of-attack range (in the neighborhood of the angles for maximum lift coefficient). Contributing to this instability were a loss in tail contribution to $C_{n\beta}$ in the high angle-of-attack range, which is discussed

in the next section, and an increase in the unstable contribution of the wing-fuselage combination to $C_{n\beta}$ over a short range of angle of attack in the high angle-of-attack range. Because of the fuselage, the wing-fuselage combination, with tail on or off, produced an unstable increment in $C_{n\beta}$ throughout the angle-of-attack range. In the absence of the tail the effect of the wing on directional stability was of secondary importance. In the presence of the tail the influence of the wing, however, assumed major importance at high angles of attack by reducing the tail contribution to $C_{n\beta}$. At high angles of attack the unswept-wing-fuselage combinations of reference 2 were directionally stable in comparison with the unstable 45° swept-wing-fuselage combinations of the present investigation. Also, the tail contributions to directional stability of the unswept models were significantly greater than those of the 45° swept-wing models.

While Reynolds number affects the effective dihedral parameter $C_{l\beta}$, the directional derivative $C_{n\beta}$ seems to be relatively free of scale effects. (See ref. 13.)

The 45° sweptback-wing models used in this investigation did not exhibit the hysteresis effects reported for the unswept aspect-ratio-2 model of reference 2 although several attempts were made to determine the presence of hysteresis by starting the sideslip motion of the model at positive and negative sideslip angles well outside the envelope angles indicated in reference 2.

Tail contribution to static lateral stability.—The discussion herein of the tail contribution to static lateral stability is restricted principally to directional stability. The tail contribution to directional stability $(C_{n\beta})_{VH}$ was obtained by subtracting the tail-off configuration $C_{n\beta}$ from the corresponding tail-on configuration $C_{n\beta}$. For example, $C_{n\beta}$ of the complete model minus $C_{n\beta}$ of the wing-fuselage combination gives the tail contribution as affected by the wing-fuselage combination. In equation form:

$$(C_{n\beta})_{WFVH} - (C_{n\beta})_{WF} = (C_{n\beta})_{VH}$$

A decrease in the stable contribution of the tail at high angles of attack was one of the sources of directional instability of the complete models, as mentioned in the previous section. This reduction and an increased stable contribution of the tail in the presence of the wings without the fuselage at angles of attack from approximately 4° to the

neighborhood of 16° (fig. 15) are a result of the downward movement of the tail with respect to the vortex flow issuing from the swept wings. An additional possible source of influence on the tail contribution to directional stability is the variation in dynamic pressure in the region of the tail (ref. 12). At moderate angles of attack increased positive $(C_{n\beta})_{VH}$ is a result of the favorable sidewash at the tail due to the vortex flow from the wing; whereas, at high angles of attack decreased positive and even negative $(C_{n\beta})_{VH}$ is a result of unfavorable sidewash.

At high angles of attack the higher aspect-ratio wings inflict greater losses in tail contribution to directional stability than do the lower aspect-ratio wings, either with or without the fuselage.

The fuselage exerted a destabilizing influence on the tail contribution at low and moderate angles of attack with and without a wing present (fig. 13). At high angles of attack, however, the fuselage had somewhat of a stabilizing effect on the tail. Also, the addition of the fuselage to the wing-tail combination produced a stabilizing effect on the tail contribution to directional stability at high angles of attack (fig. 15). As shown in reference 6, the fuselage shape has a very definite effect on the influence of the fuselage on the tail contribution to $C_{n\beta}$.

CONCLUSIONS

Analysis of the results of an investigation to determine the effect of wing aspect ratios 2, 4, and 6 on the static longitudinal and static lateral stability characteristics of a series of 45° sweptback-midwing models through an angle-of-attack range from -4° to 32° leads to the following conclusions:

1. The tail effectiveness in producing negative pitching moment increased with an increase in wing aspect ratio and angle of attack and became approximately equal to the wing-off value at very high angles of attack.

2. All complete models tested became directionally unstable in the high angle-of-attack range primarily because of an increasing loss in the stable contribution of the tail both with angle of attack and increasing wing aspect ratio and, also, because of the unstable contribution of the wing-fuselage combination.

Langley Aeronautical Laboratory,
National Advisory Committee for Aeronautics
Langley Field, Va., June 4, 1957.

REFERENCES

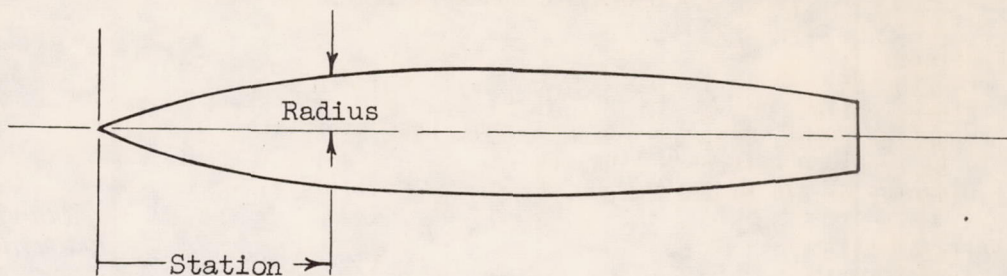
1. Campbell, John P., and McKinney, Marion O.: Summary of Methods for Calculating Dynamic Lateral Stability and Response and for Estimating Lateral Stability Derivatives. NACA Rep. 1098, 1952. (Supersedes NACA TN 2409.)
2. Wolhart, Walter D., and Thomas, David F., Jr.: Static Longitudinal and Lateral Stability Characteristics at Low Speed of Unswept-Midwing Models Having Wings With an Aspect Ratio of 2, 4, or 6. NACA TN 3649, 1956.
3. Goodman, Alex: Effects of Wing Position and Horizontal-Tail Position on the Static Stability Characteristics of Models With Unswept and 45° Sweptback Surfaces With Some Reference to Mutual Interference. NACA TN 2504, 1951.
4. Queijo, M. J., and Wolhart, Walter D.: Experimental Investigation of the Effect of Vertical-Tail Size and Length and of Fuselage Shape and Length on the Static Lateral Stability Characteristics of a Model With 45° Sweptback Wing and Tail Surfaces. NACA Rep. 1049, 1951. (Supersedes NACA TN 2168.)
5. Lichtenstein, Jacob H.: Experimental Determination of the Effect of Horizontal-Tail Size, Tail Length, and Vertical Location on Low-Speed Static Longitudinal Stability and Damping in Pitch of a Model Having 45° Sweptback Wing and Tail Surfaces. NACA Rep. 1096, 1952. (Supersedes NACA TN's 2381 and 2382.)
6. Letko, William, and Williams, James L.: Experimental Investigation at Low Speed of Effects of Fuselage Cross Section on Static Longitudinal and Lateral Stability Characteristics of Models Having 0° and 45° Sweptback Surfaces. NACA TN 3551, 1955.
7. Toll, Thomas A., and Queijo, M. J.: Approximate Relations and Charts for Low-Speed Stability Derivatives of Swept Wings. NACA TN 1581, 1948.
8. Queijo, M. J., and Riley, Donald R.: Calculated Subsonic Span Loads and Resulting Stability Derivatives of Unswept and 45° Sweptback Tail Surfaces in Sideslip and in Steady Roll. NACA TN 3245, 1954.
9. Shortal, Joseph A., and Maggin, Bernard: Effect of Sweepback and Aspect Ratio on Longitudinal Stability Characteristics of Wings at Low Speeds. NACA TN 1093, 1946.

10. Hopkins, Edward J.: Lift, Pitching Moment, and Span Load Characteristics of Wings at Low Speed As Affected by Variations of Sweep and Aspect Ratio. NACA TN 2284, 1951.
11. Salmi, Reino J., and Carros, Robert J.: Longitudinal Characteristics of Two 47.7° Sweptback Wings With Aspect Ratios of 5.1 and 6.0 at Reynolds Numbers Up to 10×10^6 . NACA RM L50A04, 1950.
12. Salmi, Reino J., and Fitzpatrick, James E.: Yaw Characteristics and Sidewash Angles of a 42° Sweptback Circular-Arc Wing With a Fuselage and With Leading-Edge and Split Flaps at a Reynolds number of 5,300,000. NACA RM L7I30, 1947.
13. Neely, Robert H., and Conner, D. William: Aerodynamic Characteristics of a 42° Swept-Back Wing With Aspect Ratio 4 and NACA 64₁-112 Airfoil Sections at Reynolds Numbers From 1,700,000 to 9,500,000. NACA RM L7D14, 1947.
14. Silverstein, Abe, and White, James A.: Wind-Tunnel Interference With Particular Reference to Off-Center Positions of the Wing and to the Downwash at the Tail. NACA Rep. 547, 1936.
15. Gillis, Clarence L., Polhamus, Edward C., and Gray, Joseph L., Jr.: Charts for Determining Jet-Boundary Corrections for Complete Models in 7- by 10-Foot Closed Rectangular Wind Tunnels. NACA WR L-123, 1945. (Formerly NACA ARR L5G31.)

TABLE I.- GEOMETRIC CHARACTERISTICS OF MODELS

Fuselage:				
Length, ft				3.750
Finess ratio				7.50
Mounting point, distance measured from nose of fuselage parallel to fuselage reference line, ft				2.125
Diameter at $\bar{c}/4$ of tail group, ft				0.170
Vertical tail:				
Aspect ratio				1.4
Sweep angle of quarter-chord line, deg				45
Taper ratio				0.6
Span, ft				0.688
Root chord, ft				0.614
Tip chord, ft				0.368
Mean aerodynamic chord, \bar{c}_v , ft				0.502
\bar{x}_v , ft				0.468
\bar{z}_v , ft				0.315
Area ratio, S_v/S_w				0.15
NACA airfoil section in planes parallel to fuselage center line				65A008
Horizontal tail:				
Aspect ratio				2.77
Sweep angle of quarter-chord line, deg				45
Taper ratio				0.60
Span, ft				1.117
Root chord, ft				0.504
Tip chord, ft				0.303
Mean aerodynamic chord, \bar{c}_h , ft				0.412
\bar{x}_h , ft				0.382
\bar{y}_h , ft				0.256
Area ratio, S_h/S_w				0.20
NACA airfoil section in planes parallel to plane of symmetry				65A008
Wings:		2	4	6
Aspect ratio				
Sweep angle of quarter-chord line, deg	45	45	45	
Taper ratio	0.60	0.60	0.60	
Span, ft	2.122	3.000	3.674	
Area, S_w , sq ft	2.250	2.250	2.250	
Root chord, ft	1.326	0.938	0.765	
Tip chord, ft	0.795	0.563	0.459	
Mean aerodynamic chord, \bar{c}_w , ft	1.083	0.766	0.625	
\bar{x}_w , ft	0.823	0.922	1.033	
\bar{y}_w , ft	0.486	0.688	0.842	
Dihedral angle, deg	0	0	0	
Twist, deg	0	0	0	
NACA airfoil section in planes parallel to plane of symmetry	65A008	65A008	65A008	

TABLE II.- FUSELAGE AND NACA 65A008 AIRFOIL ORDINATES



Fuselage ordinates	
Station, in.	Radius, in.
0	0
2.00	0.64
4.00	1.20
6.00	1.68
8.00	2.09
10.00	2.42
12.00	2.67
14.00	2.85
16.00	2.96
18.00	3.00
20.00	2.99
22.00	2.97
24.00	2.93
26.00	2.87
28.00	2.79
30.00	2.70
32.00	2.60
34.00	2.47
36.00	2.33
38.00	2.18
40.00	2.01
42.00	1.82
44.00	1.61
45.00	1.50

Ordinates of NACA 65A008 airfoil section	
Station, percent c	Ordinate, percent c
0	0
0.50	0.62
0.75	0.75
1.25	0.95
2.50	1.30
5.00	1.75
7.50	2.12
10.00	2.43
15.00	2.93
20.00	3.30
25.00	3.59
30.00	3.79
35.00	3.93
40.00	4.00
45.00	3.99
50.00	3.90
55.00	3.71
60.00	3.46
65.00	3.14
70.00	2.76
75.00	2.35
80.00	1.90
85.00	1.43
90.00	0.96
95.00	0.49
100.00	0.02

Leading-edge radius: 0.408 percent c

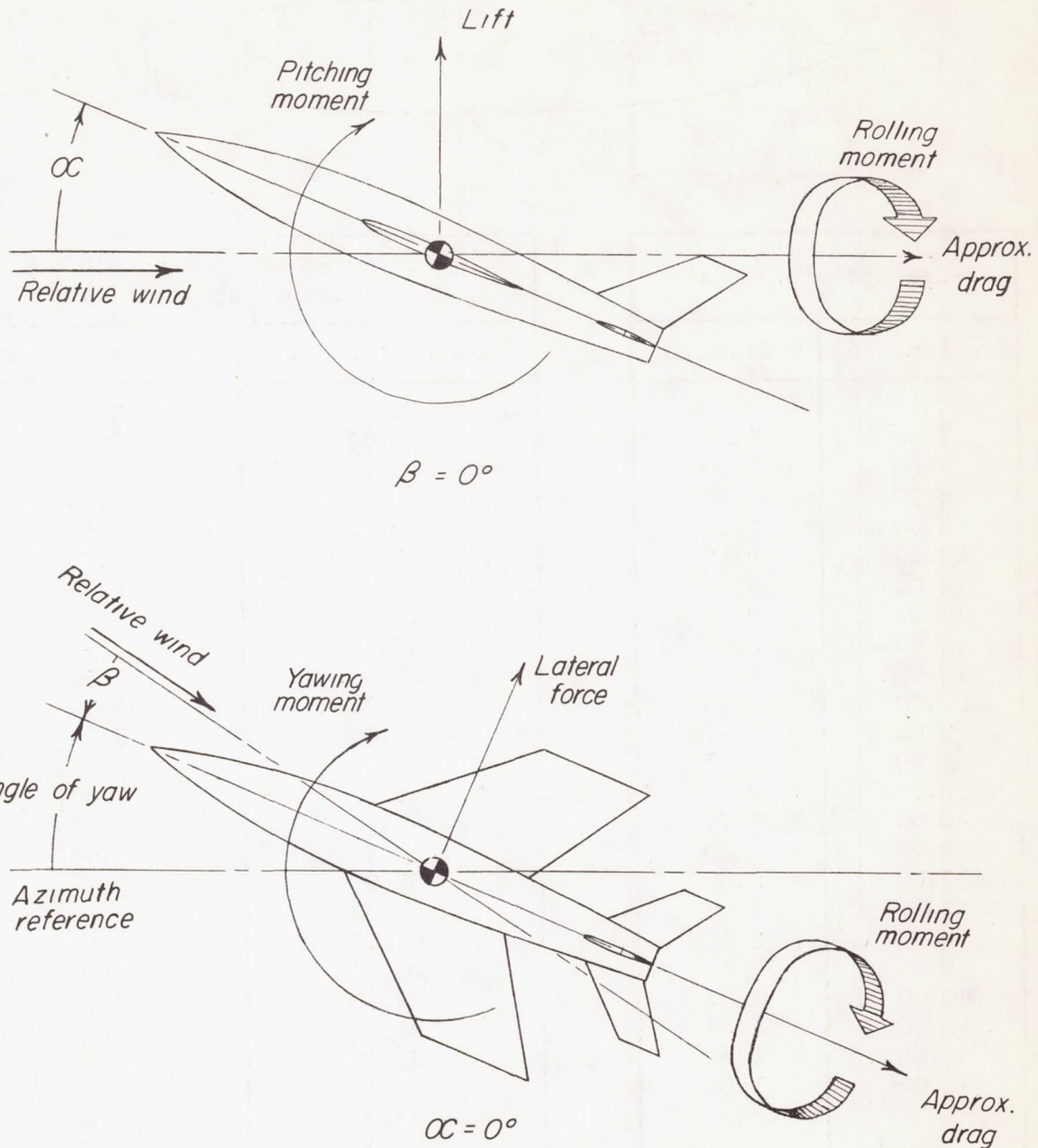


Figure 1.- Stability axes. Arrows indicate positive directions of forces, moments, and angular displacements.

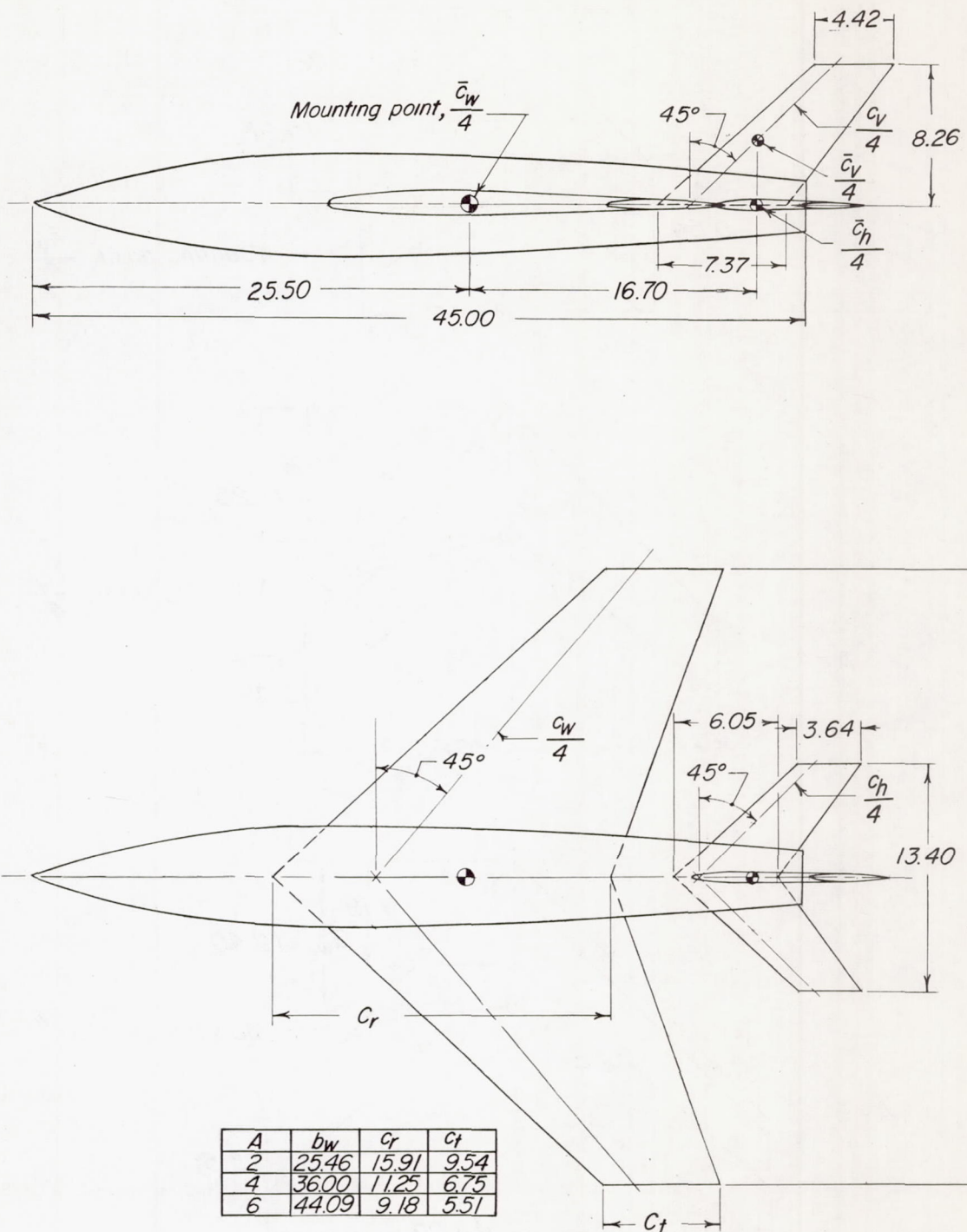


Figure 2.- General arrangement of models. All dimensions are in inches.

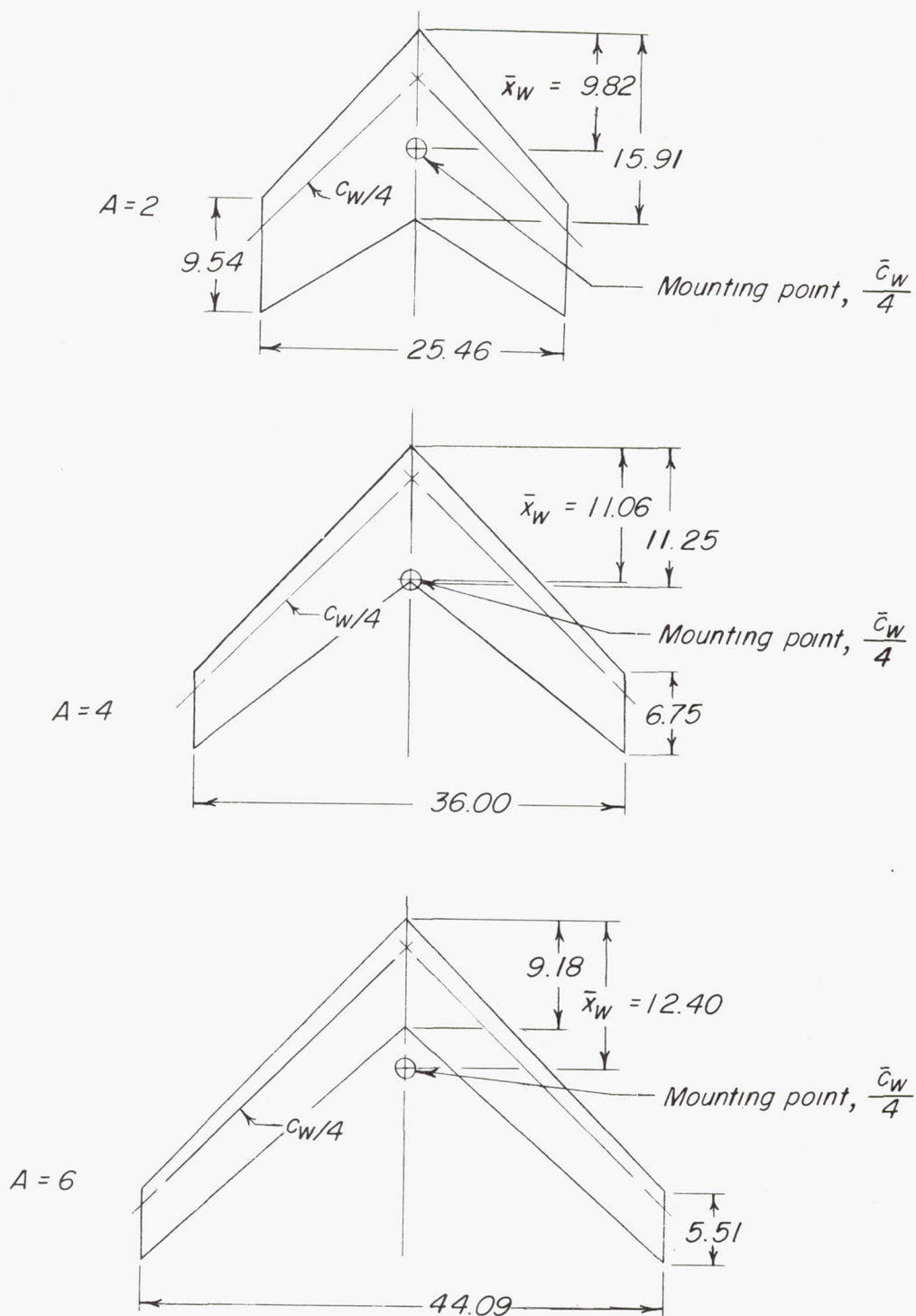
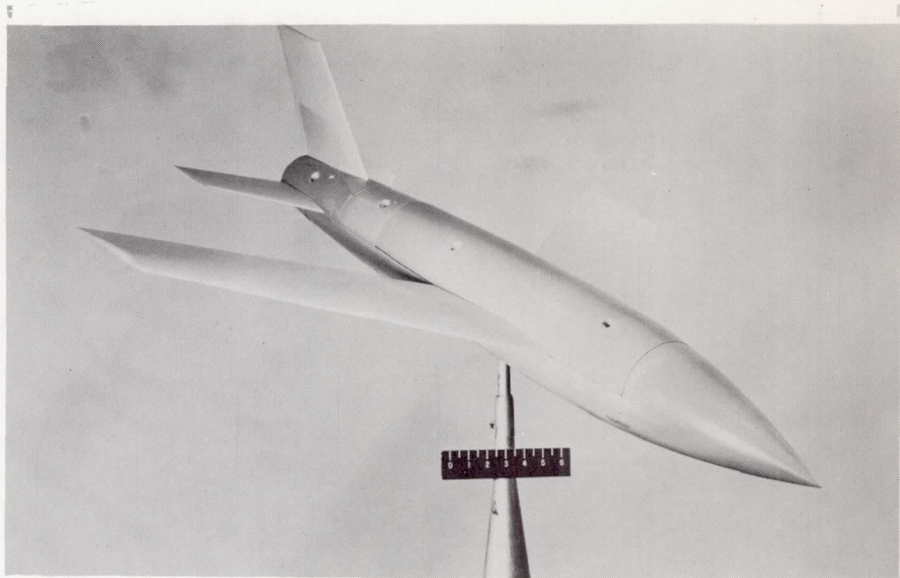
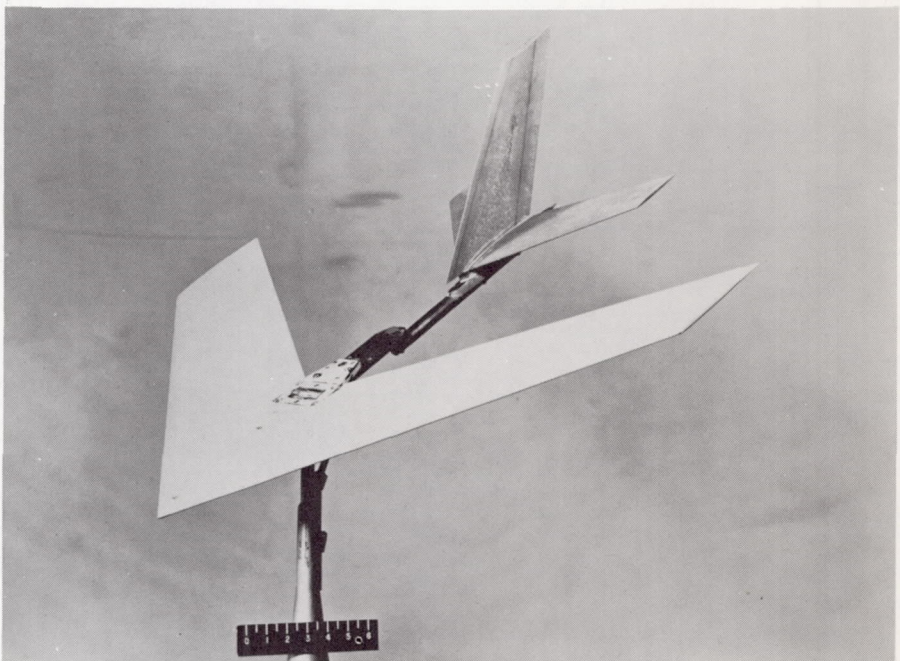


Figure 3.- Geometric characteristics of wings. All dimensions are in inches.



(a) Complete model, aspect-ratio-4 wing. L-82960



(b) Wing-tail configuration, aspect-ratio-4 wing. L-82958

Figure 4.- Two model configurations tested.

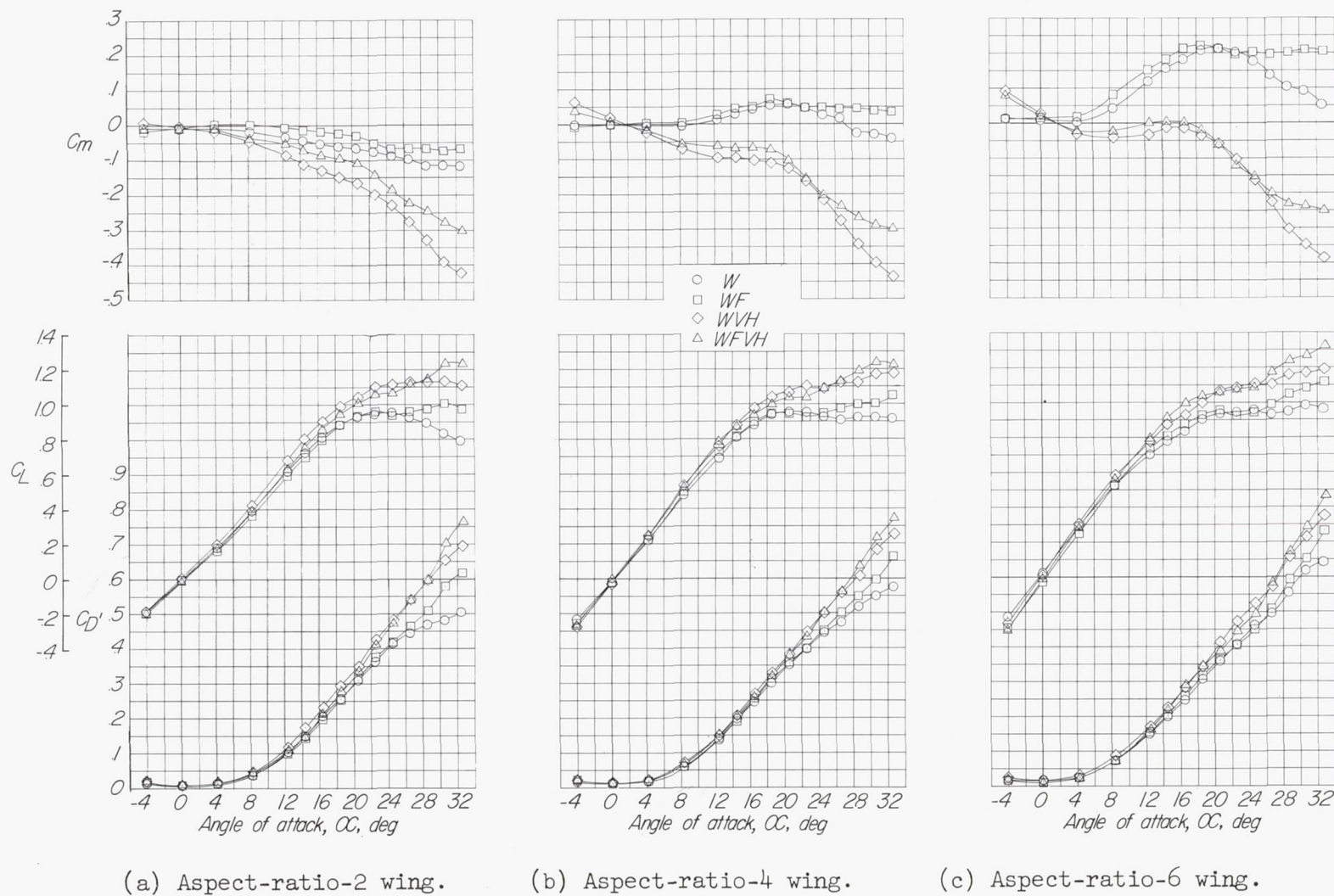


Figure 5.- Static longitudinal stability characteristics of the wing alone and in various combinations with the fuselage and tails.

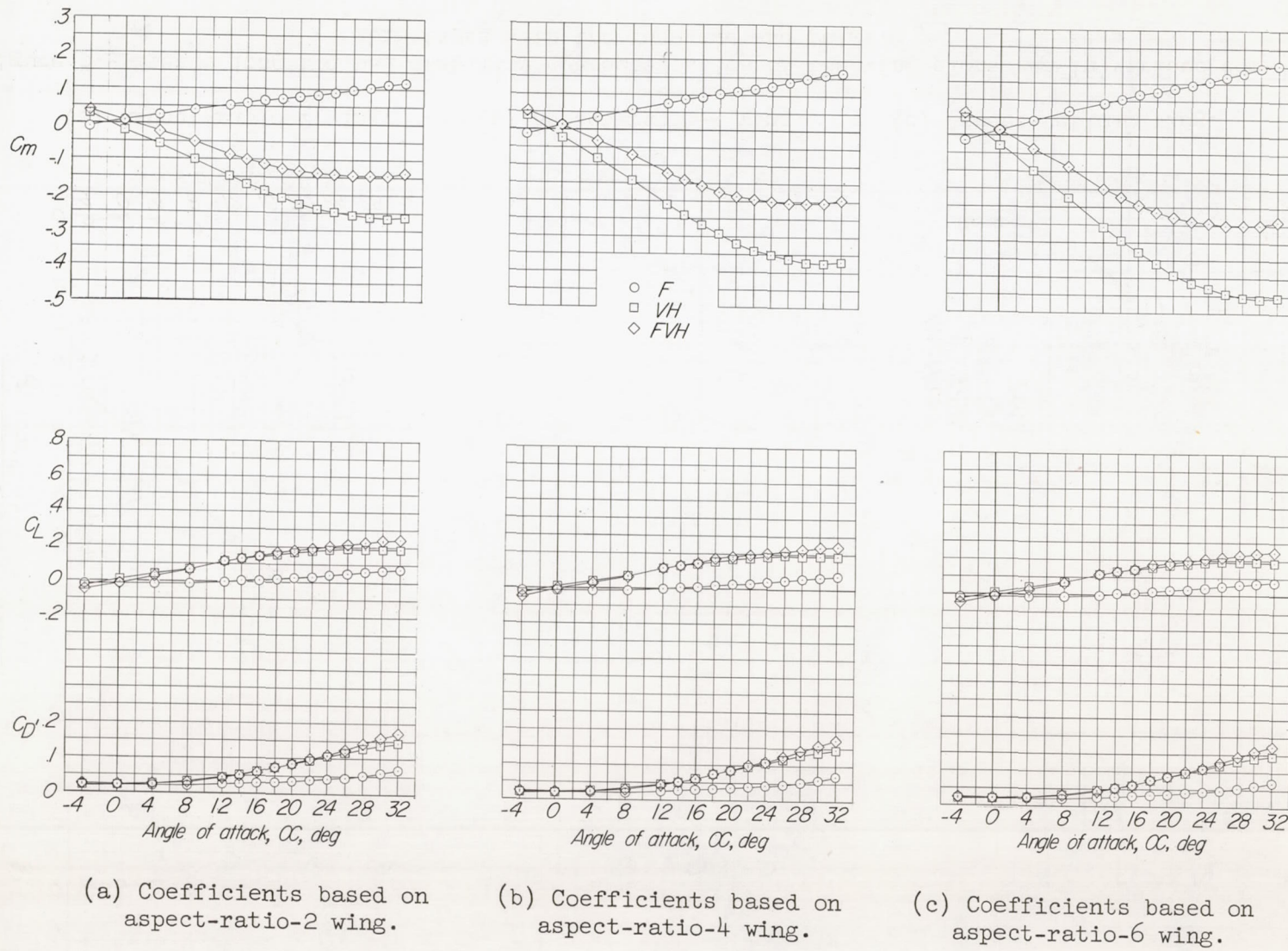


Figure 6.- Static longitudinal stability characteristics of the fuselage alone, tail alone, and fuselage-tail combination.

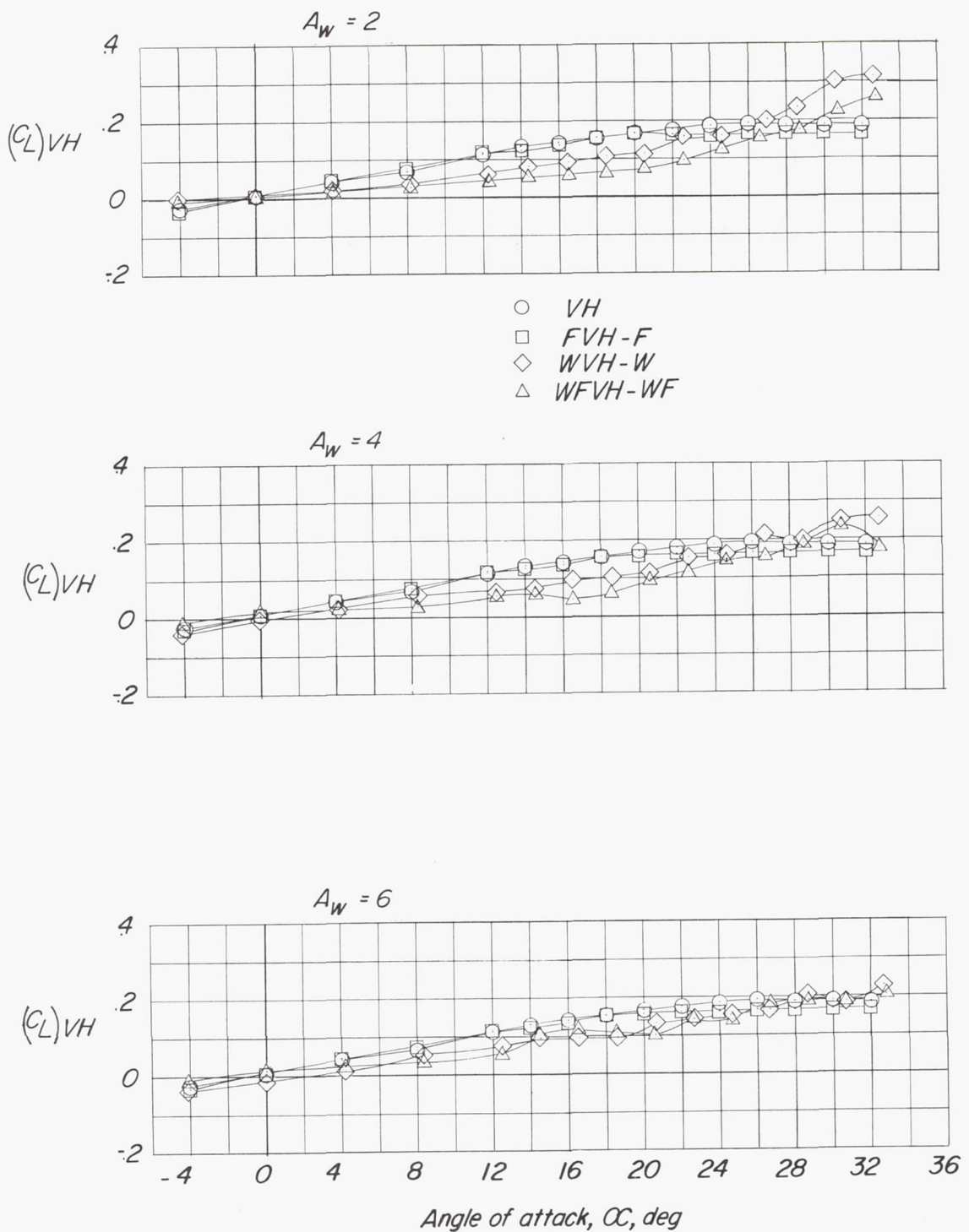


Figure 7.- Effect of the various components on the tail contribution to C_L .

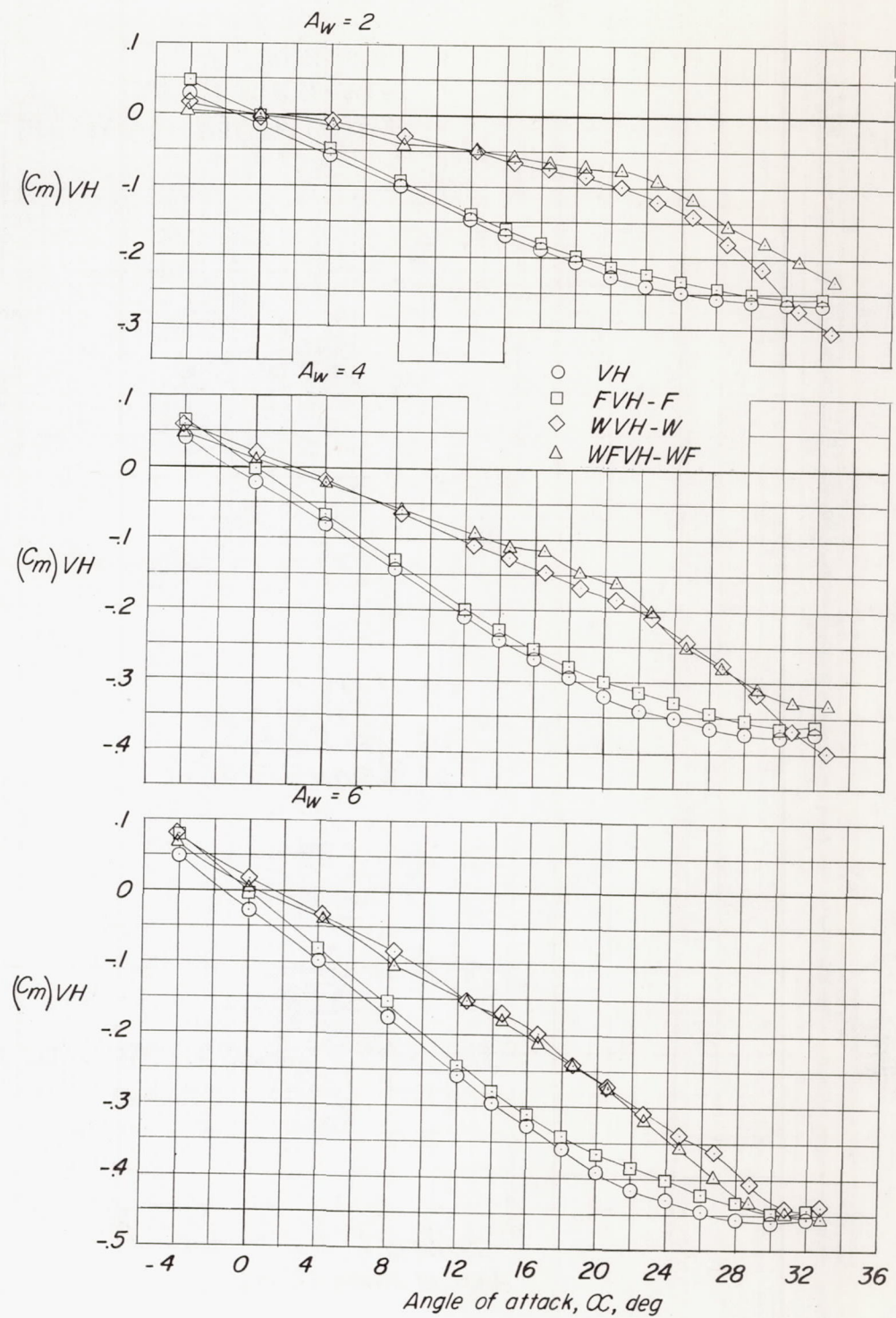


Figure 8.- Effect of the various components on the tail contribution to C_m .

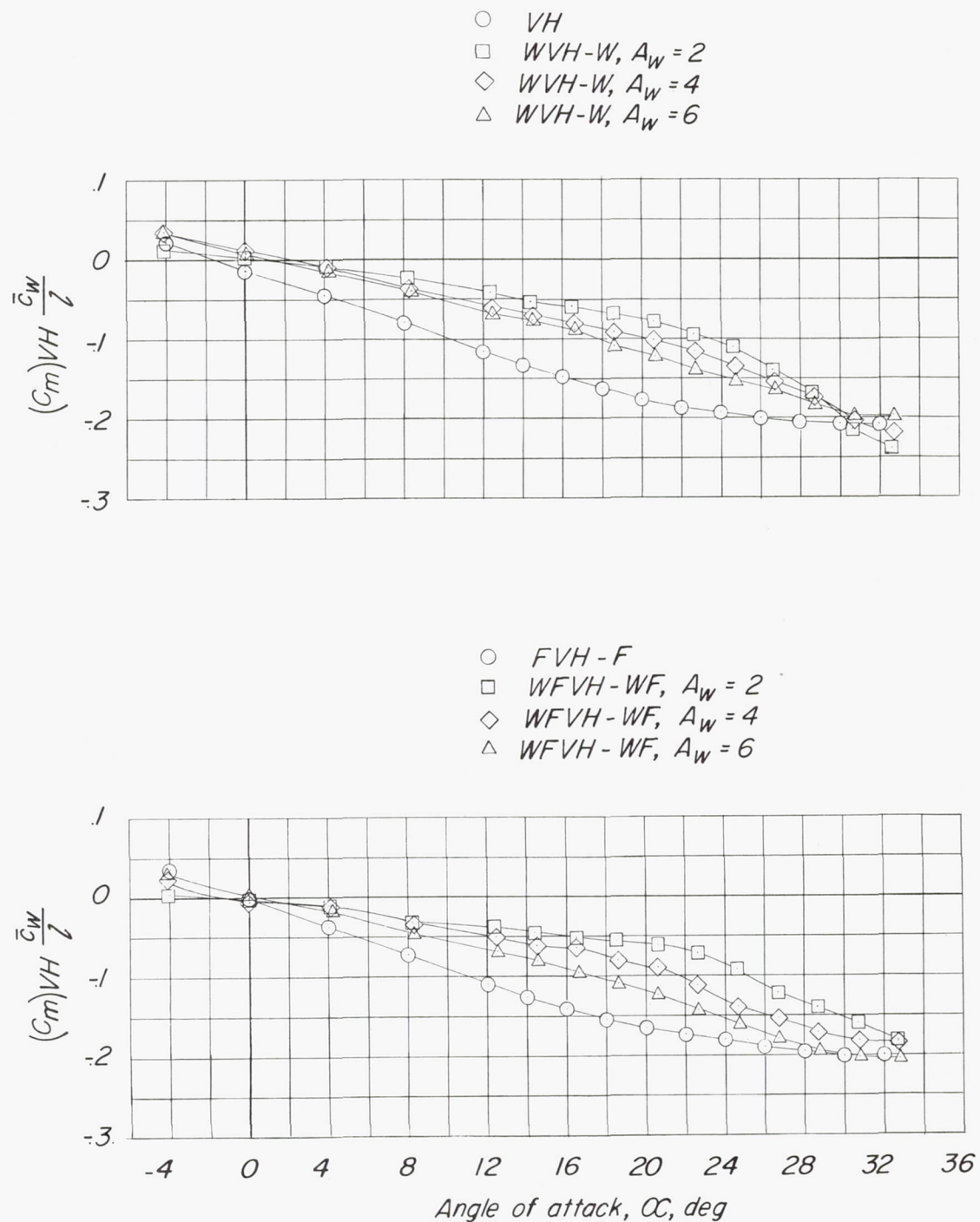


Figure 9.- Effect of wing aspect ratio on the variation of $(C_m)VH \frac{\bar{c}_w}{l}$ with α .

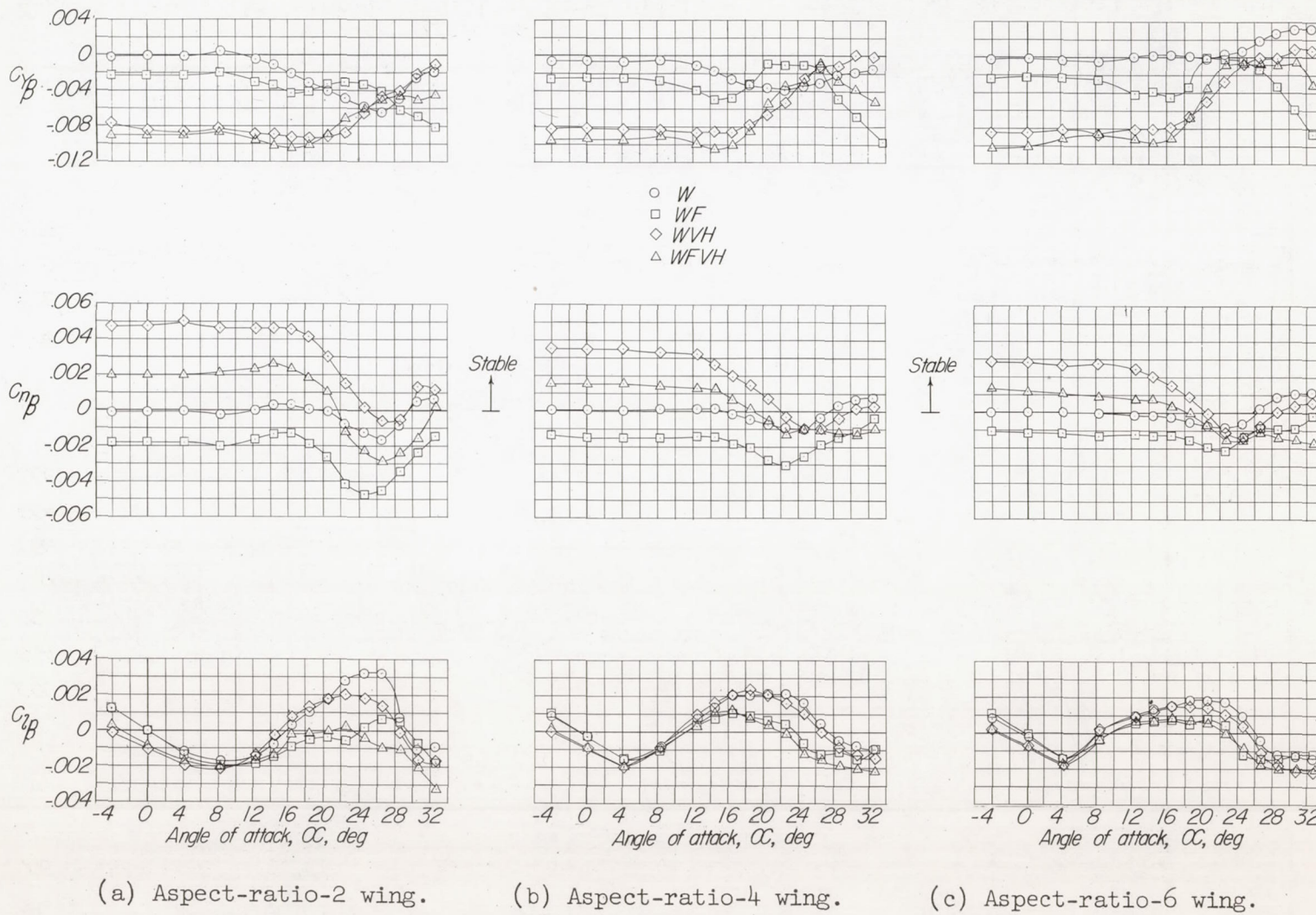


Figure 10.- Static lateral stability characteristics of the wing alone and in various combinations with the fuselage and tails.

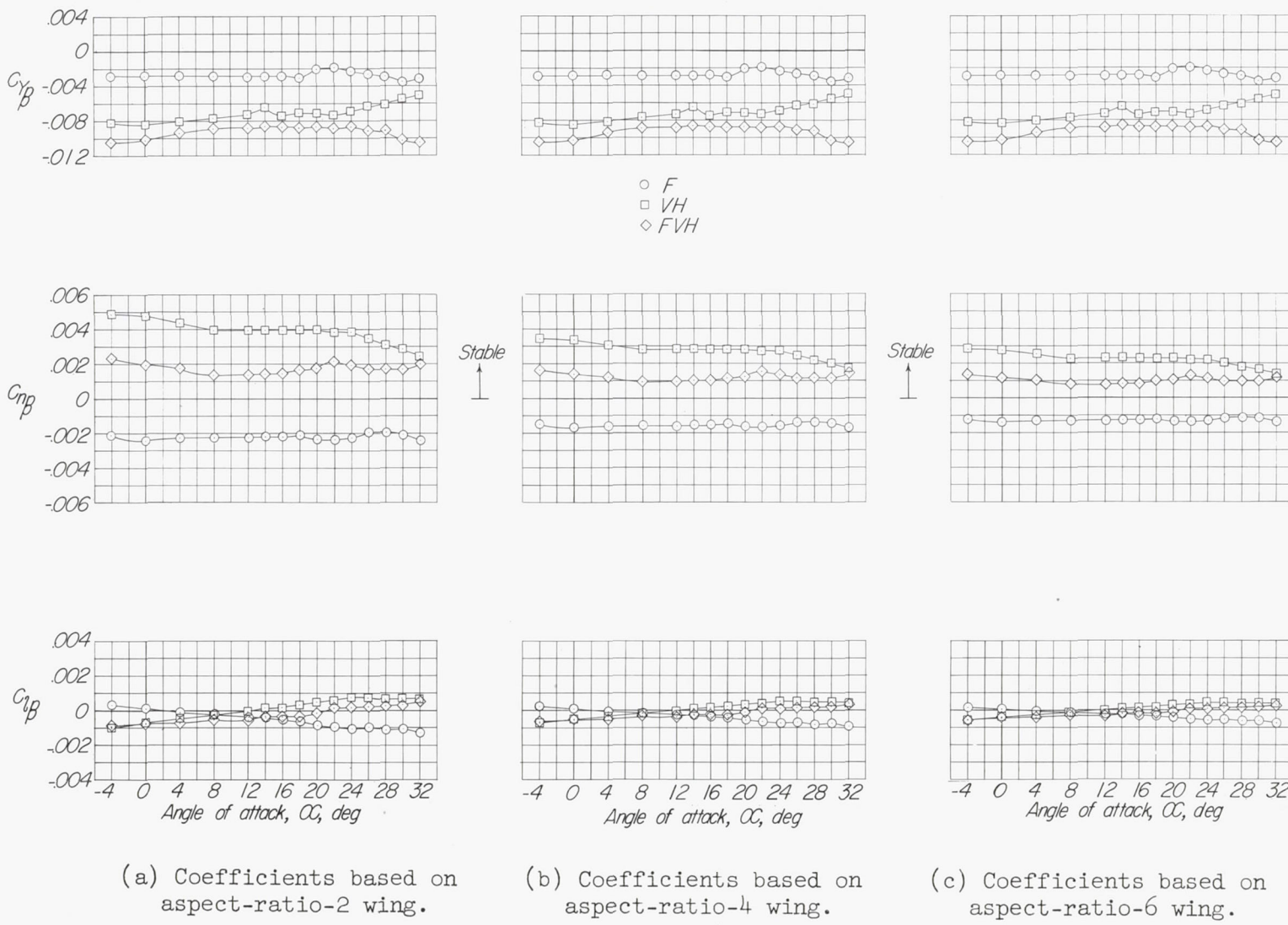


Figure 11.- Static lateral stability characteristics of the fuselage alone, tail alone, and fuselage-tail combination.

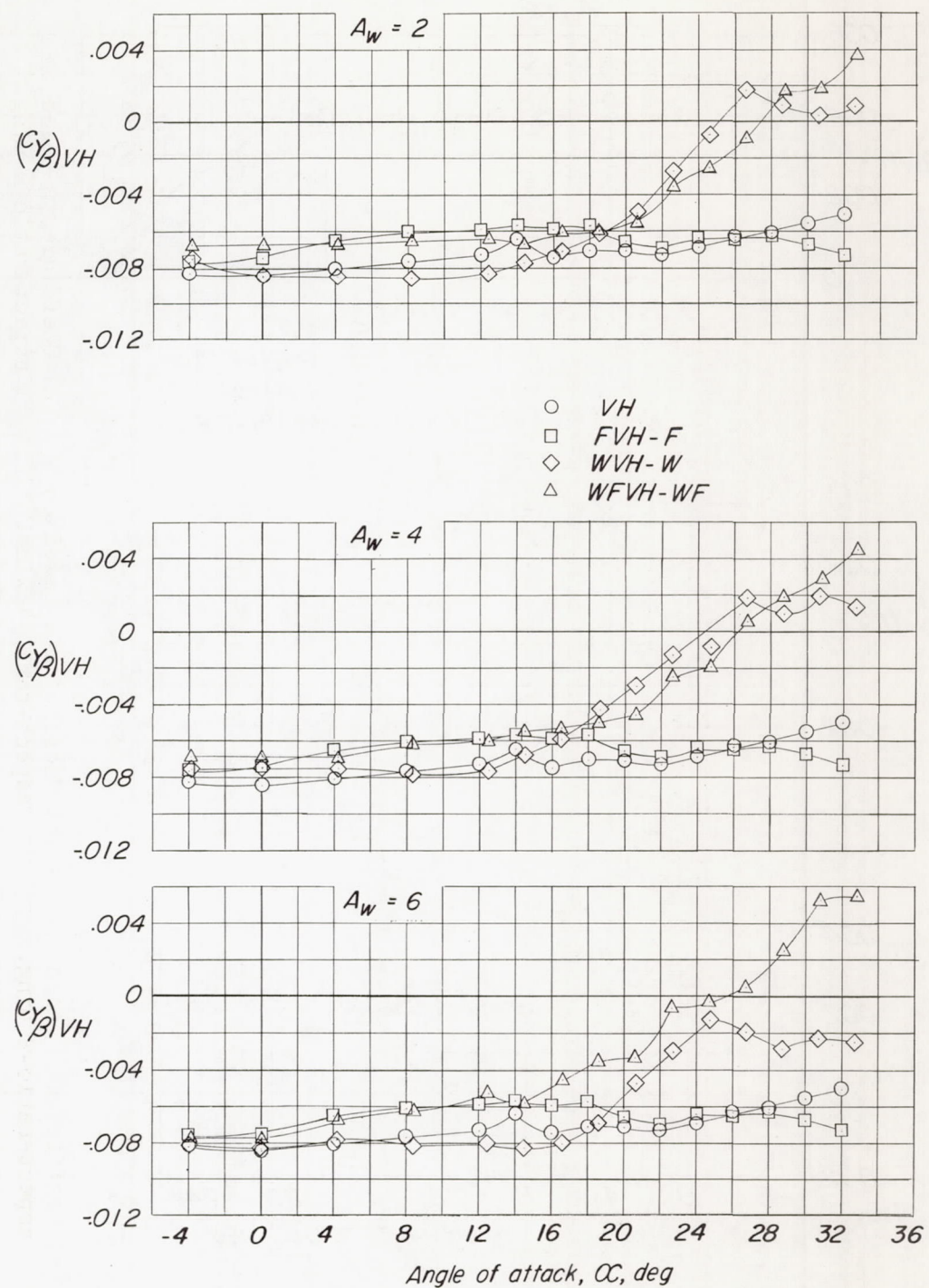


Figure 12.- Effect of the various components on the tail contribution to C_y_β .

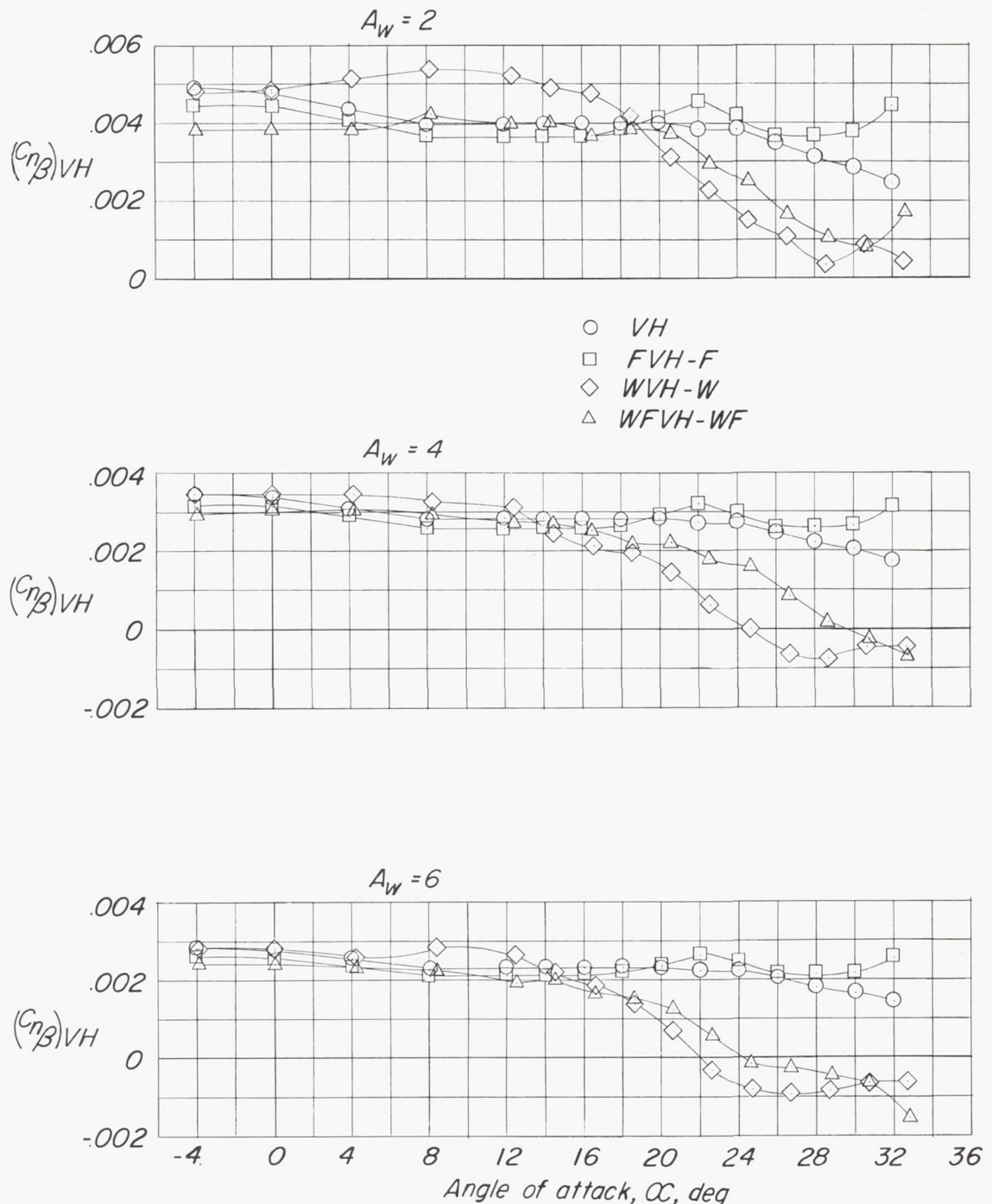


Figure 13.- Effect of the various components on the tail contribution to $C_{n\beta}$.

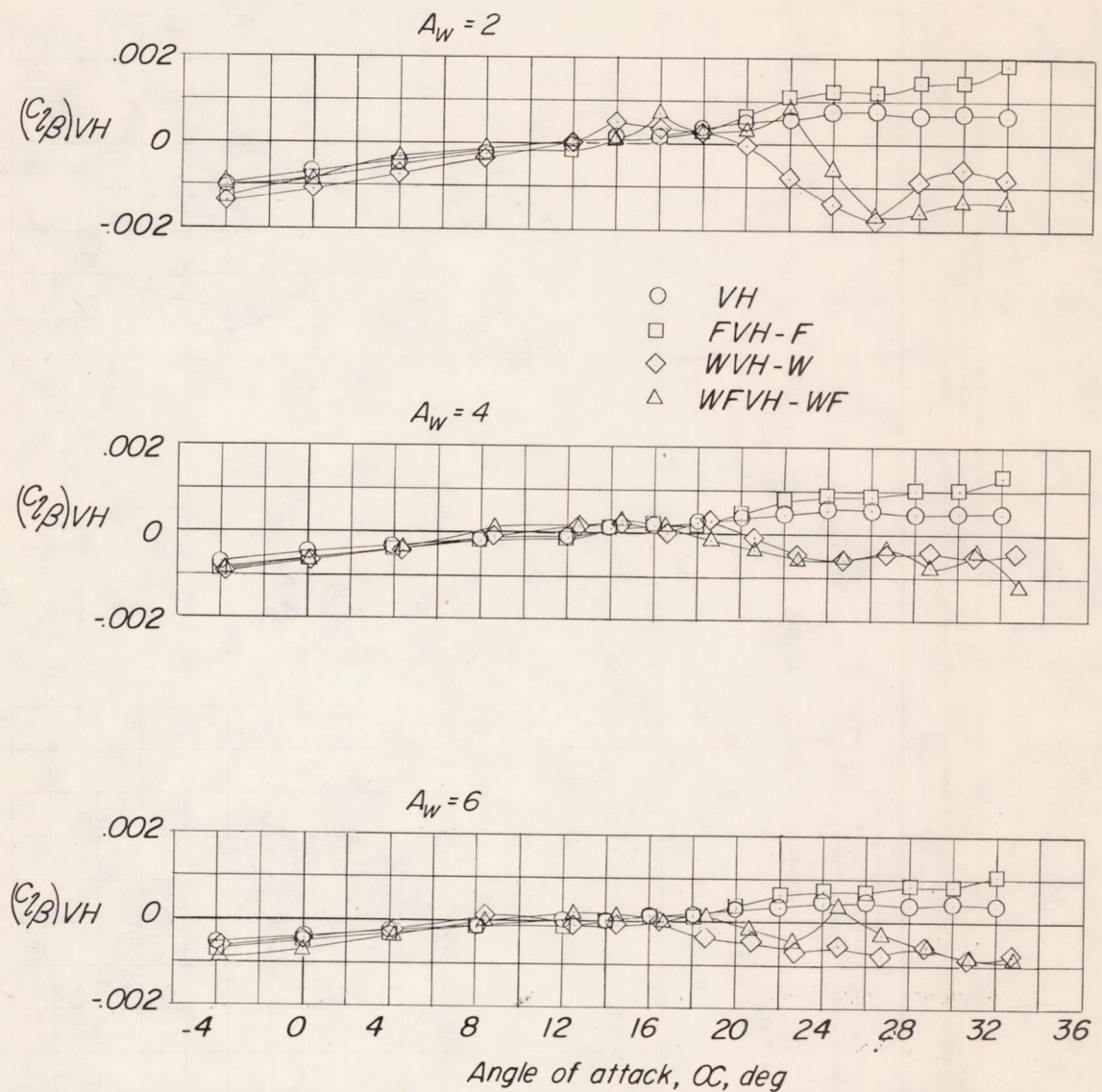


Figure 14.- Effect of the various components on the tail contribution to $C_l\beta$.

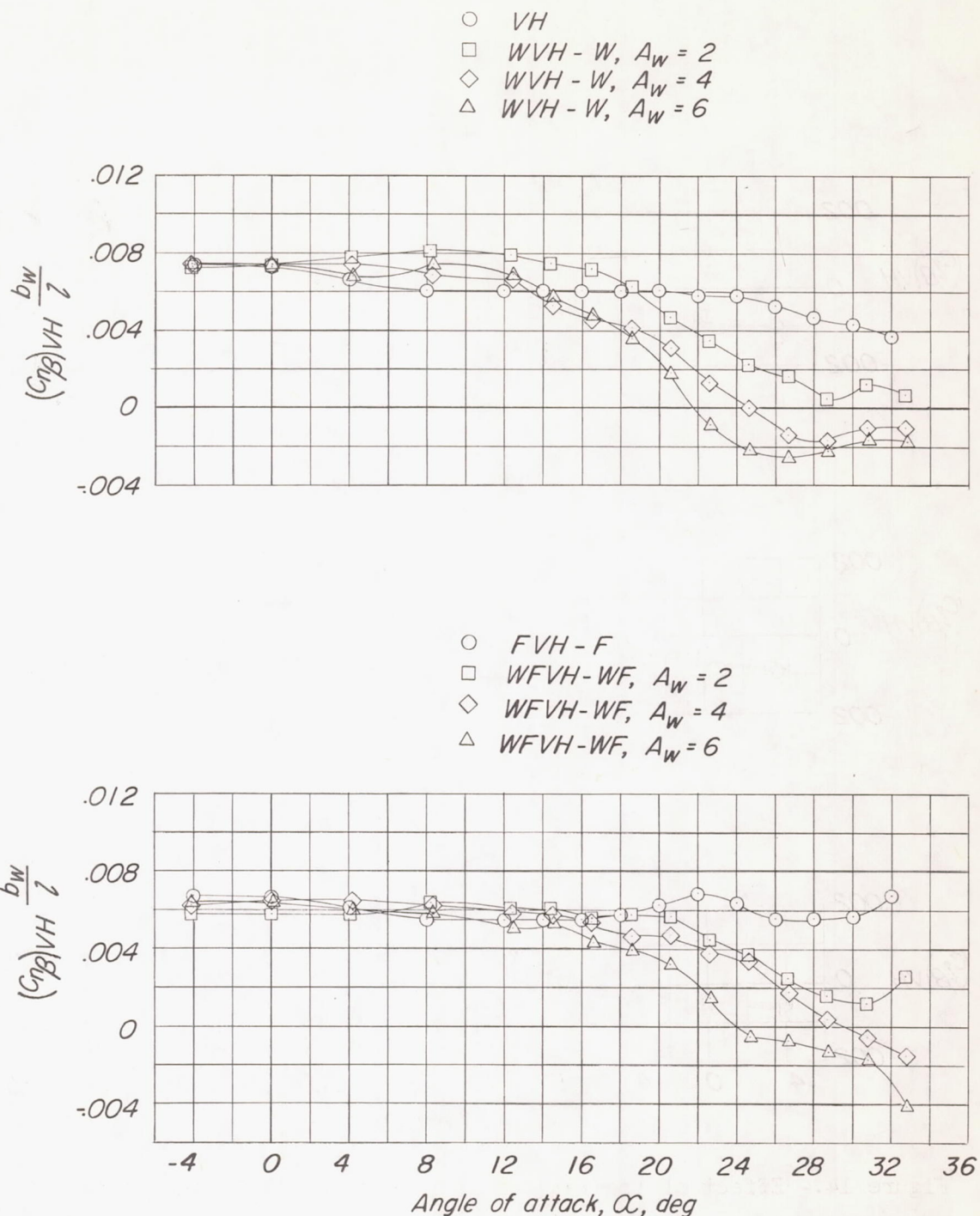


Figure 15.- Effect of wing aspect ratio on the variation of $(C_{n\beta})_{VH} \frac{b_w}{l}$ with α .